SPANDIDOS PUBLICATIONS

EXPERIMENTAL AND THERAPEUTIC MEDICINE 16: 2219-2228, 2018

Protective effects of primary neural stem cell treatment in ischemic stroke models

XIAOWEN YU[1*], XIAOQING WANG[2*], SHUXIONG ZENG[3*] and XIPING TUO[1]

Departments of [1]Gerontology, [2]Neurology and [3]Urology, Changhai Hospital, The Second Military Medical University, Shanghai 200433, P.R. China

Received October 18, 2016; Accepted August 10, 2017

DOI: 10.3892/etm.2018.6466

Abstract. Strokes are a major cause of neurological disability. Stem cell replacement therapy is a potential novel strategy of treating patients that have experienced strokes. The present study examined the protective role of neural stem cell (NSC) administration in oxygen-glucose deprivation (OGD) injury and ischemic stroke animal models. Primary cultured embryonic NSCs and brain microvascular endothelial cells were indirectly co-cultured for *in vitro* testing. A rat model of embolic middle cerebral artery occlusion (MCAO) was used to assess the morphological and functional changes that occur following treatment with NSCs. The role of the phosphoinositide 3-kinase/protein kinase b/glycogen synthase kinase 3β (PI3K/Akt/GSK-3β) signaling pathway in the neuroprotective effects of NSC treatment was also determined. It was demonstrated *in vivo* and *in vitro* that NSC administration may attenuate the brain injury caused by stroke. Furthermore, the results suggest that activation of PI3k/Akt/GSK-3β signaling pathway serves a role in attenuating OGD injury. Inflammation, synaptic remodeling and autophagy may be improved following NSC treatment and behavioral testing suggests that treatment with NSCs improves functional recovery in rats following MCAO.

Introduction

Stroke is the third-leading cause of mortality in developed countries with an incidence of 250-400 cases per 100,000 people and a mortality rate of ~30% (1). The prevalence and cost of stroke are expected to rise as the global population ages and in less developed countries, the incidence and mortality rates of stroke are increasing due to rapidly changing lifestyles and population structures (2).

Correspondence to: Professor Xiping Tuo, Department of Gerontology, Changhai Hospital, The Second Military Medical University, 168 Changhai Road, Shanghai 200433, P.R. China
E-mail: xptuo001@126.com

[*]Contributed equally

Key words: oxygen-glucose deprivation, ischemic stroke, neural stem cell, treatment

Ischemic cerebral infarction is the cause of ~80% of strokes (3). Ischemic stroke occurs following the obstruction of blood vessels supplying blood to the brain. Due to the limited regeneration capacity of central nervous tissue, patients with brain damage resulting from ischemic stroke suffer from lifelong disabilities (4).

Stem cell therapy is a potential novel strategy of treating patients that have experienced strokes. It has been demonstrated to have therapeutic potential in animal models of neurological disorders (5,6). Previous studies have also performed cell transplantation in models of ischemic infarct. Different types of stem cells, including rodent mesenchymal stem cells (7), human bone marrow stem cells (8), human umbilical cord blood cells (9) and rodent embryonic hippocampal formation cells (10) ameliorate neurological deficits induced by experimental brain ischemia. The present study investigated the effects of primary rodent neural stem cell (NSC) administration on *in vitro* and *in vivo* stroke models and determined the role of the phosphoinositide 3-kinase/protein kinase b/glycogen synthase kinase 3β (PI3K/Akt/GSK-3) signaling pathway in the neuroprotective effects of pre-treatment with NSCs.

Materials and methods

Primary culture of NSCs. Complete NSC medium was prepared by mixing Neuralbasal medium (20 ml/brain; Thermo Fisher Scientific, Inc., Waltham, MA, USA) with 10 ng/ml B27 (Invitrogen; Thermo Fisher Scientific, Inc.), 10 ng/ml basic fibroblast growth factor and 20 ng/ml epidermal growth factor (both Gibco; Thermo Fisher Scientific, Inc.). The dissociated brain tissue from one animal was then diluted in 20 ml of culture medium. The mixture was supplemented with 1% antibiotics (penicillin/streptomycin) and incubated at 37˚C with 5% CO_2 and 95% humidity.

A dissection microscope (Fisher Science Education™ Advanced Digital Stereomicroscopes; cat. no. S71012B; Thermo Fisher Scientific, Inc.) was used to harvest Sprague-Dawley rat embryos at day 13 (E13; the copulatory plug day was defined as E0). Rats (age, 3-5 weeks; weight, 250±30 g) were obtained from Changhai Hospital Animal Center (Shanghai, China) and housed under controlled environmental conditions (temperature, 23±1˚C; humidity, 55±5% and kept under a 12 h light/dark cycle; commercial food and water were freely available). Trypsin (0.25%) was used to homogenize whole brain

samples (obtained from rat embryos). Neurospheres were cultured as described previously (11). Cells were incubated at 37˚C with 5% CO_2. NSCs were identified using immunofluorescence labeling with anti-nestin antibody (1:1,000; cat. no. 14-9843-82; Thermo Fisher Scientific, Inc.) and were then passaged for three generations prior to administration.

Primary culture of brain microvascular endothelial cells (BMECs). Rat BMECs were isolated from Sprague-Dawley rats, following a previously published protocol with some modifications (12). Briefly, rat brains were collected and homogenates of isolated cerebral cortices were then digested using 0.1% collagenase II (Sigma-Aldrich; Merck KGaA, Darmstadt, Germany) and 30 U/ml DNase I (cat. no. 10104159001; Roche Diagnostics, Indianapolis, IN, USA) at 37˚C for 1.5 h. The pellet was then resuspended in 20% bovine serum albumin (BSA; Sigma-Aldrich; Merck KGaA; 2 ml) and centrifuged at 1,000 x g for 20 min at 4˚C. Microvessel pellets in the lower layer were digested using 0.1% collagenase/dispase (Roche Diagnostics) and 20 U/ml DNase I at 37˚C for 1 h. Cells were incubated at 37˚C with 5% CO_2 and a humidity of 95%. BMECs were identified using immunofluorescence labeling with anti-factor VIII antibody (1:1,000; cat. no. MA1-43037; Thermo Fisher Scientific, Inc.). Fluorescence microscope was used to identify cell samples.

Oxygen-glucose deprivation (OGD) cell model. A Transwell chamber (EMD Millipore, Billerica, MA, USA) indirect co-culture system was used to identify the effect of NSCs on BMECs under OGD. The groups for the OGD cell model were as follows: An NSC group, a control group and an OGD group. For the NSC group, the upper compartments of the Transwell inserts were removed following co-culture of NSCs and BMECs (each $4x10^5$/well) in Dulbecco's Modified Eagle medium (DMEM)-F12 (Thermo Fisher Scientific, Inc.) mixed with 2% B27 and 1% fetal bovine serum (Sigma-Aldrich; Merck KGaA) for 72 h at 37˚C. BMECs were treated with DMEM comprising of glucose-free balanced salt solution and cultured for 6 h in a hypoxic chamber under an adjusted atmosphere comprising of 95% N_2 and 5% CO_2 at 37˚C; the control group consisted of BMECs without NSCs that had not been exposed to OGD; and the OGD group consisted of BMECs without NSCs that had been exposed to OGD, which served as an internal control.

Animal model of middle cerebral arterial occlusion (MCAO). MCAO surgery was performed to induce focal cerebral ischemic injury. Adult male Sprague-Dawley rats aged 6-8 weeks old and weighing 250-350 g were obtained from the Second Military Medical University (SMMU) Laboratory Animal Center (Shanghai, China). Following intraperitoneal anesthesia with 10% chloral hydrate (360 mg/kg; Sigma-Aldrich; Merck KGaA), focal cerebral ischemia was induced using an operating microscope via right-sided endovascular MCAO using a piece of monofilament nylon suture with a blunted tip coated with poly-lysine. The filament was inserted through the right common carotid artery and advanced along the internal carotid artery until the tip occluded the proximal stem of the middle cerebral artery. Induction of ischemic brain injury was confirmed using behavioral tests.

Implantation of NSCs in a rat model. NSCs were collected using centrifugation (800 x g for 5 min at room temperature) and resuspended in PBS. Rats were intraperitoneally anesthetized with 10% chloral hydrate (400 mg/kg). A stereotaxic instrument was then used to fix the animal's head with the lambda point set at 0: Anteroposterior (AP)=16 mm; medial lateral (ML)=21.6 mm; dorsal ventral (DV)=12.9 mm; and hippocampus (point of NSCs administration): AP=19 mm; ML=23.6 mm; DV=14.9 mm (Read coordinate from behind, back, and top, anteroposterior=AP, medial lateral=ML, and dorsal ventral=DV). Each rat received 10 μl total fluid using microsyringes over a 10 min period immediately following MCAO. Following confirmation of the induction of ischemic brain injury using behavioral tests, rats were randomized into three groups for transplantation as follows: i) The NSC group, consisting of rats that underwent transplantation of ~$4x10^5$ NSCs into the hippocampus around the ischemic boundary zone by injection following MCAO, ii) the MCAO group, consisting of rats that underwent MCAO alone with PBS transplantation and iii) the sham group, consisting of rats that underwent MCAO without insertion of the filament into the MCA and transplantation of PBS. Mice were anesthetized by inhaling 2.5% isoflurane before Perform cervical dislocation. At 3 days after MCAO, mice were sacrificed and samples were collected for further study. All animals were treated in accordance with the NIH guidelines for the Care and Use of Laboratory Animals (13). All experimental procedures in the current study were approved by the Committee on Ethics of Biomedicine, The Second Military Medical University.

Caspase-3 activity assay. Caspase-3 is one of the key enzymes that serve a role in apoptosis. A caspase-3 colorimetric assay (Caspase 3 Activity assay kit, Colorimetric; Sigma-Aldrich; Merck KGaA) was performed, which is based on the hydrolysis of the peptide substrate acetyl-Asp-Glu-Val-Asp p-nitroanilide (Ac-DEVD-pNA) by caspase-3, a process that results in the release of the p-nitroaniline (pNA) moiety. Samples and standards were processed as indicated in the manufacturer's protocol. Cells were homogenized in lysis buffer (included in the kit) and centrifuged for 15 min at a speed of 13,400 x g at 4˚C and the supernatant was collected. The reaction was initiated by adding Ac-DEVD-pNA to each well and the mixture was shaken gently. The microplate was incubated at 37˚C for 3 h and absorbance was measured at a wavelength of 405 nm using a microplate reader.

Lactate dehydrogenase (LDH) release assay demonstrating cell cytotoxicity. Cell cytoxicity following OGD treatment was determined based on the release of LDH using the CytoTox-one Homogeneous Membrane Integrity assay kit (Promega Corporation, Madison, WI, USA) following the manufacturer's protocol. Cytotoxicity was calculated using the following formula: Cytotoxicity (%)=100x(experimental-culture medium background)/(maximum LDH release-culture medium background).

Reverse transcription-quantitative polymerase chain reaction (RT-qPCR) in brain tissue from rat models. RT-qPCR was performed as previously described to determine the expression of PI3k, Akt and GSK-3β mRNA (14). Briefly, 1 μg total RNA

was isolated using TRIzol reagent (Thermo Fisher Scientific, Inc.) and was then reverse transcribed into cDNA with a commercially available Reverse transcription kit (Tiangen Biotech, Co., Ltd., Beijing, China) following the manufacturer's protocol. qPCR was performed using a SYBR Green PCR Master mix (Tiangen Biotech, Co., Ltd.) on an ABI 7300 PCR Instrument (Applied Biosystems; Thermo Fisher Scientific, Inc.). The following primers were used: PI3K, forward, 5'-CTCTCCTGTGCTGGCTACTGT-3' and reverse, 5'-GCTCTCGGTTGATTCCAAACT-3'; Akt, forward, 5'-TCAGGATGTGGATCAGCGAGA-3' and reverse, 5'-CTGCAGGCAGCGGATGATAA-3'; GSK-3β, forward, 5'-TTCTCGGTACTACAGGGCACCA-3', and reverse, 5'-GTCCTAGCAACAATTCAGCCAACA-3' and β-actin, forward, 5'-GGAGATTACTGCCCTGGCTCCTA-3' and reverse, 5'-GACTCATCGTACTCCTGCTTGCTG-3'. The following cycling conditions were used: 10 min at 95˚C for polymerase activation, followed by 95˚C for 30 sec and 60˚C for 30 sec. Rat β-actin was used for normalization. Relative fold changes in RNA expression normalized to β-actin were calculated using the $2^{-\Delta\Delta Cq}$ method (15).

Western blot analysis. Total protein lysates from the ischemic penumbra area tissues were prepared with ice-cold lysis buffer (50 mM Tris, pH 7.6, 150 mM NaCl, 10% Triton-X 100 and 100x Roche protease inhibitor cocktail protease and phosphatase inhibitors). Brain tissues were then centrifuged in a microcentrifuge at a speed of 13,400 x g rpm for 1 min at 4˚C. Protein concentration was determined using a BCA assay kit (Promega Corporation). A total of 40 μg proteins were loaded per lane and resolved using 10% SDS-polyacrylamide gel electrophoresis for 2 h at 120 V prior to being transferred to PVDF membranes using wet tank electro transfer, membranes were blocked with 5% BSA in TBST overnight at 4˚C. Membranes were then incubated with primary antibodies against phosphorylated (p)-PI3k (1:1,000; cat no. 4228), p-Akt (1:1,000; cat no. 4060) and p-GSK3β (1:1,000; cat no. 9323; all Cell Signaling Technology, Inc., Danvers, MA, USA) in 5% BSA blocking buffer overnight at 4˚C. Membranes were also incubated with the following antibodies obtained from Abcam: PI3K (cat. no. ab86714, 1:1,000 dilution), Akt (cat. no. ab126811, 1:1,000 dilution), GSK3β (cat. no. ab18893, 1:1,000 dilution) and GAPDH (cat. no. ab8245, 1:2,000 dilution). These were then blocked using 5% skimmed milk at room temperature for 2 h. Subsequently membranes were incubated with the horseradish-peroxidase-conjugated secondary antibody (Horeseradish peroxidase conjugated-goat anti-Rabbit immunoglobulin G; 1:4,000; cat. no. AB_2533967; Thermo Fisher Scientific, Inc.) in blocking buffer for 1 h at room temperature. Samples were visualized using an ECL kit (cat. no. Ab65623; Abcam).

Quantification of inflammatory cytokines. The expression of cytokines within the brain [Leptin, L-selectin, monocyte chemotactic protein-1 (MCP-1), tissue inhibitor of metalloproteinases 1 (TIMP-1), tumor necrosis factor (TNF)-α] were measured using a Multiplexed Sandwich ELISA-based Quantitative array-quantibody Rat Cytokine Array 2 kit (cat. no. QAR-CYT-2; RayBiotech, Inc., Norcross, GA, USA). The protein molecules were quantified according to the manufacturer's protocol. A total of 5 animals per group were used for cytokine analysis.

Hematoxylin and eosin (H&E) staining. Tissue was removed and fixed immediately in 4% paraformaldehyde at room temperature for 24 h. Brain sections (4 μm) were mounted on gelatin-coated slides. Mounted sections were then rehydrated in distilled water and submerged in Hematoxylin for 5 min at room temperature. Sections were then rinsed and submerged in eosin for 2 min at room temperature. Following eosin treatment, sections were dehydrated in a graded ethanol series prior to immersion in xylene. A light microscope was used to visualize the H&E stained sections.

Nissl staining. Tissue was fixed in 4% paraformaldehyde at room temperature for 24 h. Coronal brain sections (4 μm) were mounted on gelatin-coated glass slides. Nissl assays were performed following a previously described protocol (16). Briefly, samples were rehydrated using decreasing ethanol concentrations and endogenous peroxidase activity was quenched with 2% H_2O_2. The slides were then processed for Nissl staining, according to standard protocols. A light microscope was used to visualize the Nissl stained sections (magnification, x400).

Immunohistochemistry. Immunohistochemical staining of the brain tissue samples was performed 4 days following MCAO surgery using an antigen retrieval method, following a previously described protocol (7). Brain sections were incubated with anti-microtubule-associated protein 2 (MAP-2) antibody (1:1,000; cat no. ab32454; Abcam, Cambridge, MA, USA), anti-growth associated protein-43 (GAP-43) antibody (1:1,000; cat no. ab117265; Abcam), anti-synaptophysin antibody (1:1,000; cat no. ab175533; Abcam), anti-glial fibrillary acidic protein (GFAP) antibody (1:1,000; cat no. HPA056030; Sigma-Aldrich; Merck KGaA), anti-ionized calcium binding adaptor protein (IBA-1) antibody (1:1,000; cat no. HPA056030; Sigma-Aldrich; Merck KGaA), anti-microtubule-associated protein light chain 3 (MAP1LC3A) antibody (1:1,000; cat no. SAB1306673; Sigma-Aldrich; Merck KGaA) or anti-Beclin-1 antibody (1:1,000; cat no. SAB1306484; Sigma-Aldrich; Merck KGaA) overnight at 4˚C. Brain samples were then incubated with biotinylated goat anti-rabbit immunoglobulin G (cat no. A0208; Beyotime Institute of Biotechnology, Haimen, China), followed by streptavidin-peroxidase (Beyotime Institute of Biotechnology) for 40 min at room temperature. The data were analyzed using Image J software version 1.48 (National Institutes of Health, Bethesda, MD, USA). A total of 5 animals per group were used for immunohistochemical analysis, 5 fields of the brain of each rat at x200 magnification were selected and mean optical density was calculated.

Behavioral tests. The modified foot-fault test and adhesive removal test were employed 3 days following MCAO rat model establishment, which aimed to measure forelimb placement dysfunction and somatosensory deficits, respectively (17,18). The total number of steps that the rat used to cross the grid, left forelimb foot faults and the mean time required to remove each stimulus from the limbs was recorded.

Statistical analysis. Statistical significance among the groups was analyzed using one-way analysis of variance and Tukey's

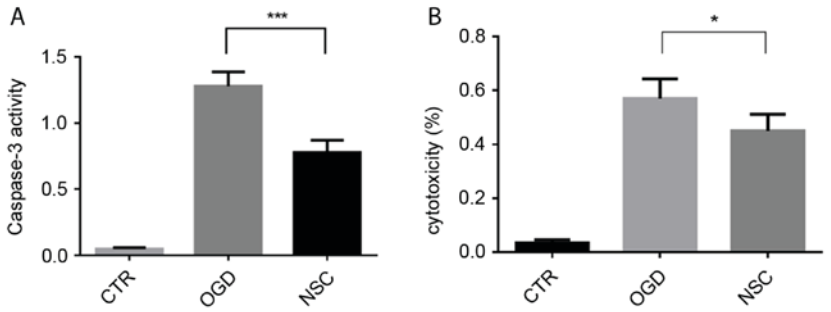

Figure 1. The effect of NSCs on caspase-3 activity and LDH release in OGD-treated BMECs. (A) BMECs were co-cultured with NSCs for 72 h prior to being subjected to OGD injury for 6 h. Apoptosis was analyzed using a caspase-3 activity assay. (B) LDH release as an indicator of % cytoxicity in OGD-treated BMECs. Data are presented as the mean ± standard deviation (n=3). ***P<0.001; *P<0.05. NSCs, neural stem cells; LDH, lactate dehydrogenase; OGD, oxygen-glucose deprivation; CTR, control; BMECs, brain microvascular endothelial cells.

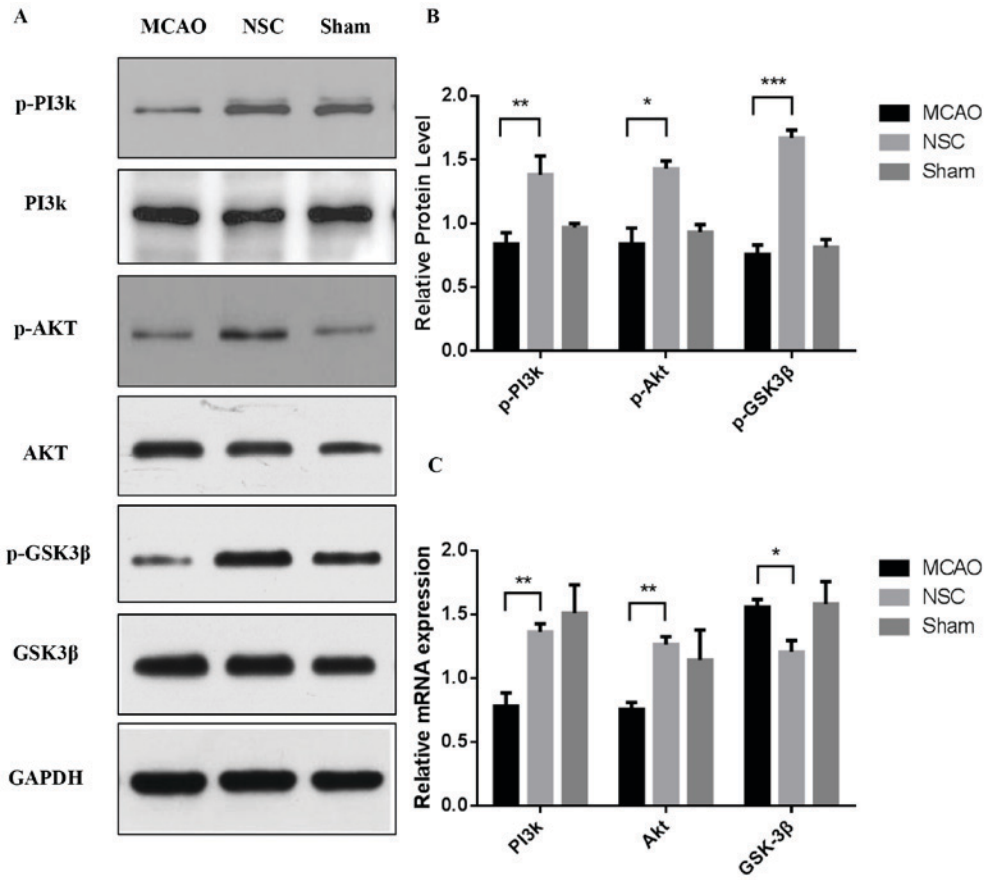

Figure 2. Western blotting and reverse transcription-quantitative polymerase chain reaction analysis of the expression of p-PI3k, p-Akt and p-GSK3β in brain tissues from an MCAO rat model. (A) Levels of p-PI3k, p-Akt and p-GSK3β protein were analyzed using western blotting and GAPDH was used as a loading control. (B) Quantitative analysis of western blotting. Expression of p-PI3k, p-Akt and p-GSK3β were normalized to total PI3k, Akt and GSK3β. (C) Quantitative analysis of the relative levels of PI3k, Akt and GSK3β mRNA. Data are presented as the mean ± standard deviation. All experiments were performed in triplicate. *P<0.05, **P<0.01, ***P<0.001. p-, phosphorylated; PI3k, phosphoinositide 3-kinase; Akt, protein kinase b; GSK3β, glycogen synthase kinase 3β; MCAO, middle cerebral artery occlusion group; NSC, neural stem cell group.

post hoc test. Data are expressed as the mean ± standard deviation. P<0.05 was determined to indicate statistically significant difference. Statistical analysis was performed using SPSS 19.0 (IBM Corp., Armonk, NY, USA).

Results

NSCs significantly suppress caspase-3 activity and decrease the release of LDH in BMECs. Caspase-3 activation serves a key role in apoptosis and may be used as a marker of apoptosis. Caspase-3 activity was increased ~1.4-fold in the OGD group compared with the NSC group (P<0.001; Fig. 1A). LDH is an indicator of cytotoxicity, which is released into the cell culture supernatant when cell membranes are damaged. The effect of NSCs on OGD-induced BMEC cytotoxicity was evaluated using an LDH release assay (Fig. 1B). The cytotoxicity of the NSC group was significantly decreased compared with the OGD group (P<0.05).

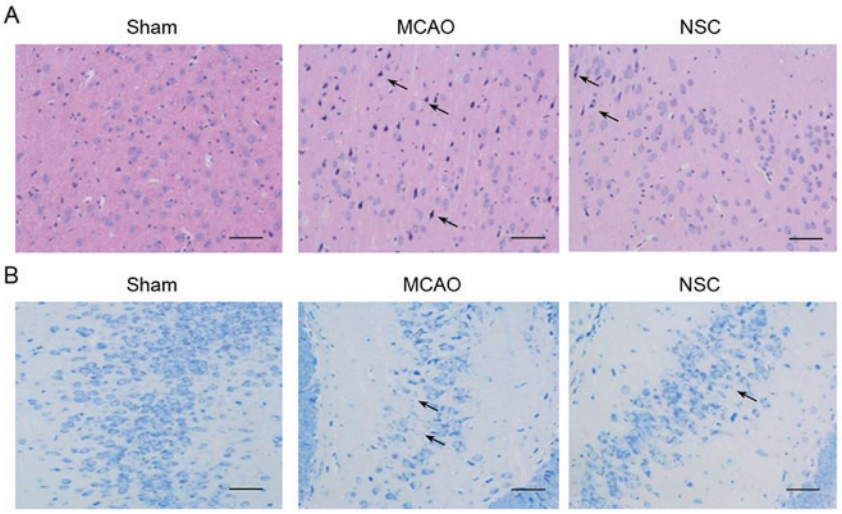

Figure 3. H&E and Nissl staining in brain tissues from an MCAO rat model. (A) H&E staining in the dentate gyrus of the hippocampus. Arrows indicate ambiguous structures and nuclear shrinkage. (B) Nissl staining in adjacent hippocampal sections. Arrows indicate Nissl staining loss. Scale bar=50 μm. Magnification, x200. MCAO, middle cerebral artery occlusion group; NSC, neural stem cell group; H&E, hematoxylin and eosin.

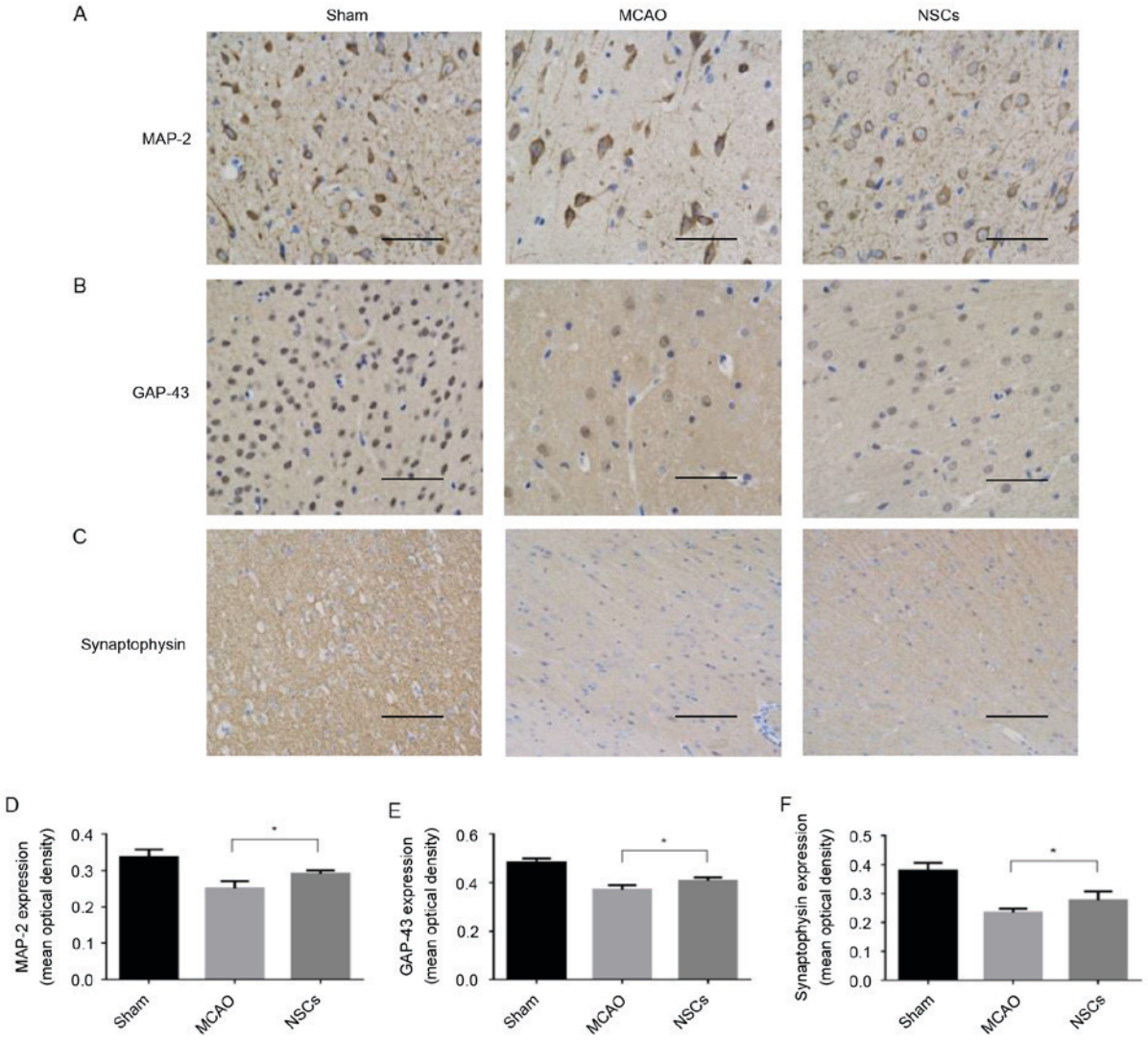

Figure 4. Synaptic remodeling mediated by NSCs in brain tissue from an MCAO rat model. (A) Immunofluorescence staining of GAP-43. (B) Immunofluorescence staining of MAP-2. (C) Immunofluorescence staining of synaptophysin. (D) Mean optical density of MAP-2 expression in brain samples. (E) Mean optical density of GAP-43 expression in brain samples. (F) Mean optical density of synaptophysin expression in brain samples. Data are presented as the mean ± standard deviation (n=5). *P<0.05. Scale bar=50 μm. Magnification, x200. MCAO, middle cerebral artery occlusion group; NSCs, neural stem cells; MAP-2, anti-microtubule-associated protein 2; GAP-43, anti-growth associated protein-43.

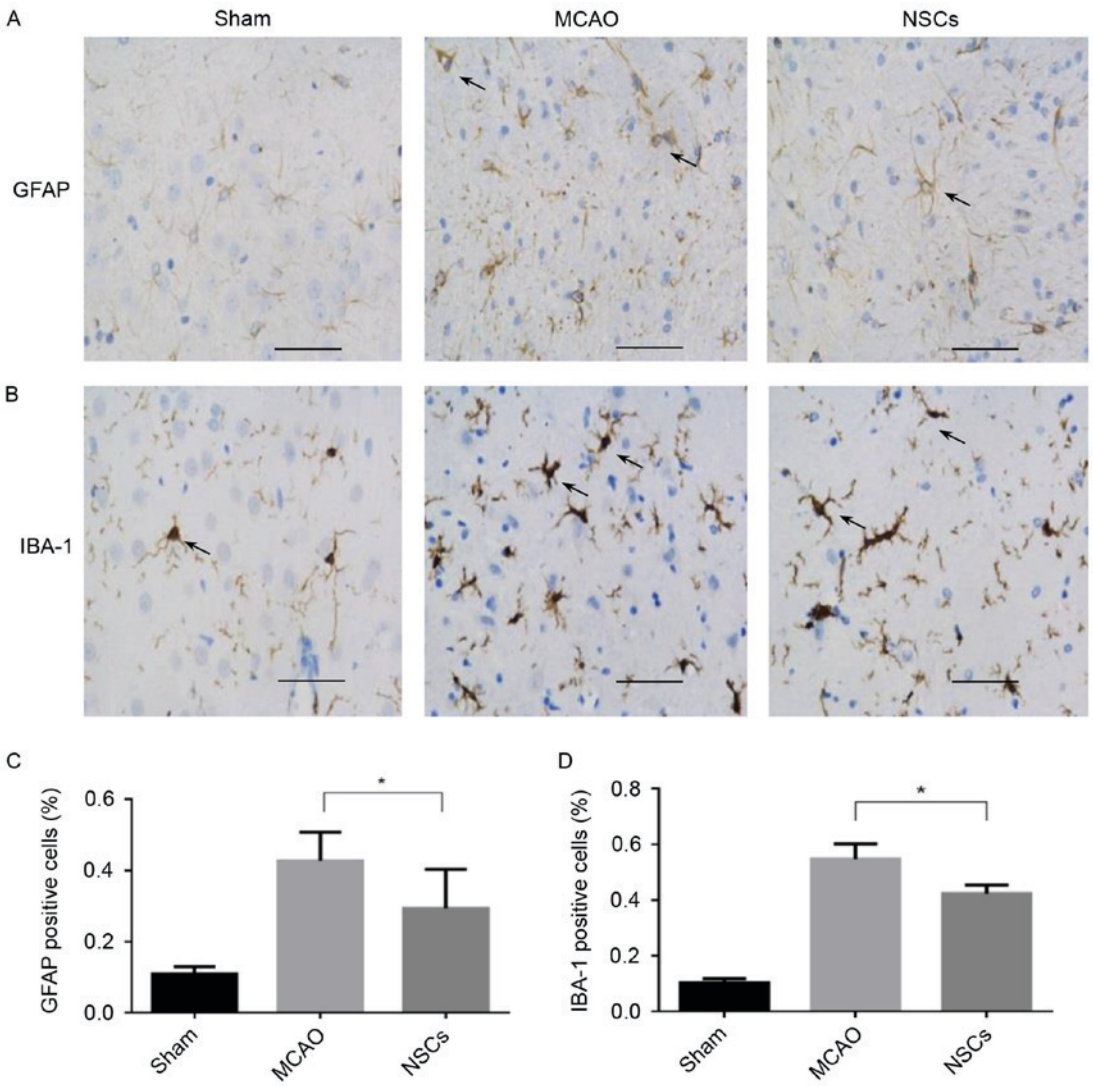

Figure 5. The effect of NSC treatment on immunoreactive cells from the brain tissue of rats that underwent MCAO. (A) Immunofluorescence staining of GFAP. Arrows indicate GFAP positive cells. (B) Immunofluorescence staining of IBA-1. Arrows indicate IBA-1 positive cells. (C) Percentage of GFAP positive cells. (D) Percentage of IBA-1 positive cells. Data are presented as the mean ± standard deviation (n=5). *P<0.05. Scale bar=50 μm. Magnification, x200. MCAO, middle cerebral artery occlusion group; NSC, neural stem cell group; GFAP, anti-glial fibrillary acidic protein; IBA-1, anti-ionized calcium binding adaptor protein.

Effects of NSCs on PI3k/Akt/GSK-3β signaling pathway activation. Our previous *in vitro* study demonstrated that phosphorylation levels of PI3k/Akt/GSK-3β were altered in neurons following NSCs treatment under OGD (unpublished data). The results of the *in vivo* experiments in the current study further indicated that the PI3k/Akt/GSK-3β signaling pathway may be at least partially involved in the neuroprotective effects conferred by NSCs. The expression of p-PI3k, p-Akt and p-GSK3β protein was measured using western blotting (Fig. 2A). The expressions of p-PI3k at Tyr458 (P<0.01), p-Akt at Ser473 (P<0.05) and p-GSK-3β at Ser9 (P<0.001) were significantly increased in the NSC group compared with the MCAO group (Fig. 2B) RT-qPCR analysis was performed simultaneously to measure the level of expression of PI3k, Akt and GSK-3β mRNA (Fig. 2C). The results indicated that the levels of PI3k and Akt mRNA were increased in the NSC group compared with the MCAO group (both P<0.01). By contrast, the expression of GSK-3β mRNA was significantly decreased (P<0.05) in the NSC group compared with the MCAO group.

H&E and Nissl staining. The results of H&E staining of the dentate gyrus of the hippocampus in the MCAO group identified the following typical neuropathological changes in rats: Neuronal cell loss, ambiguous structures, nuclear shrinkage and dark neuron staining. NSC treatment significantly attenuated these ischemic neuropathological changes (Fig. 3A). The adjacent hippocampal sections were subjected to Nissl staining (Fig. 3B). The reduction in Nissl staining is indicative of neuronal degeneration. A greater reduction of Nissl staining was evident in the tissues from the MCAO group compared with tissues from the NSC group.

Synaptic remodeling is mediated by NSCs in the MCAO animal model. MAP-2 is a cytoskeletal phosphoprotein primarily associated with microtubules and postsynaptic densities (19). GAP-43 is an intracellular membrane-associated phosphoprotein expressed in neuronal growth cones and is involved in axonal growth, synaptogenesis, synaptic remodeling and neurotransmitter release (20). Synaptophysin is a 38-kDa calcium-binding glycoprotein present in the membranes of

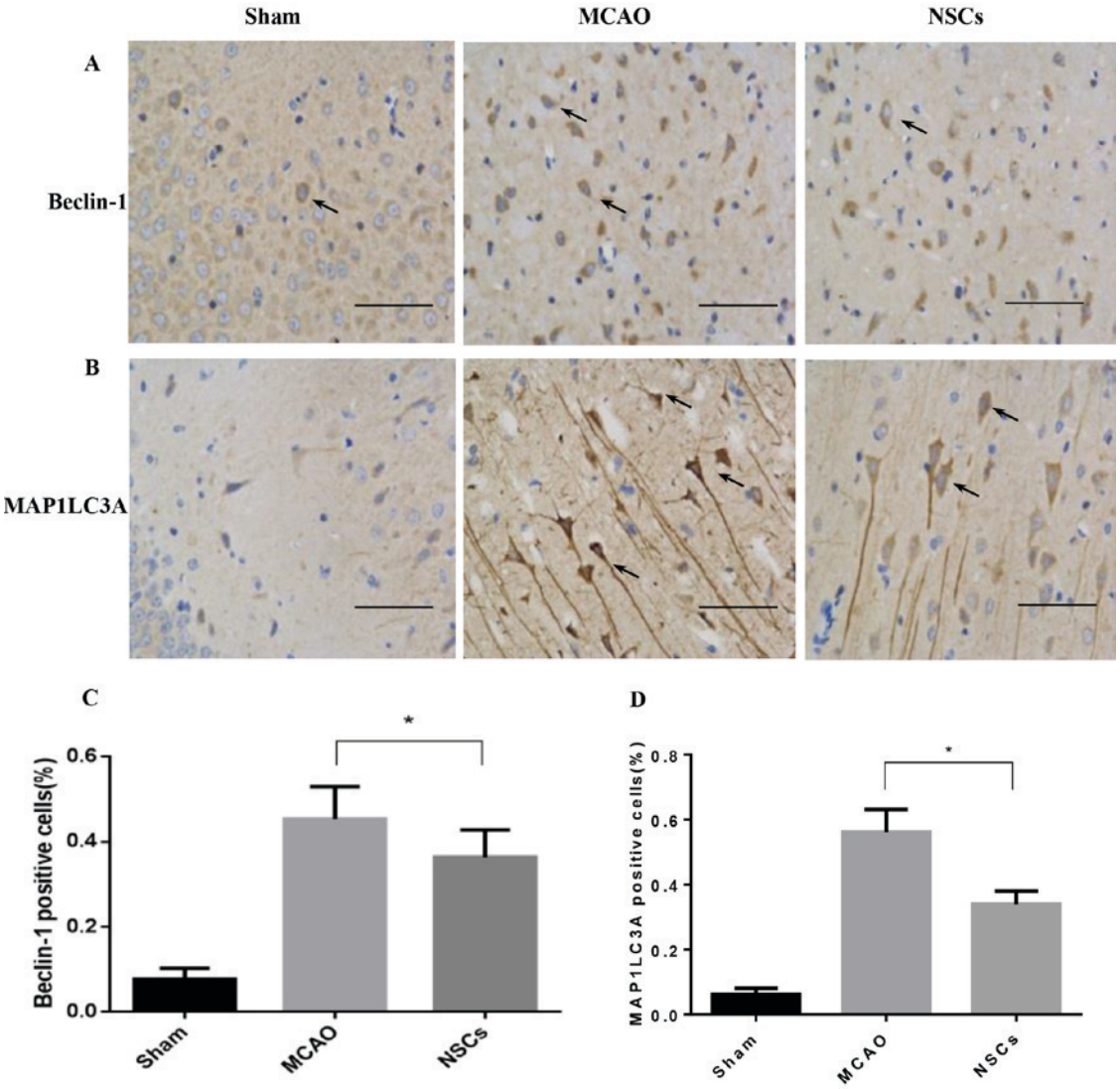

Figure 6. Markers of autophagy are decreased following NSC treatment in the brain tissues of rats that underwent MCAO. (A) Immunofluorescence staining of Beclin-1. Arrows indicate Beclin-1 positive cells. (B) Immunofluorescence staining of MAP1LC3A. Arrows indicate MAP1LC3A positive cells. (C) Percentage of Beclin-1 positive cells. (D) Percentage of MAP1LC3A positive cells. Data are presented as the mean ± standard deviation (n=5). *P<0.05. Scale bar=50 μm. Magnification, x200. MCAO, middle cerebral artery occlusion group; NSCs, neural stem cell group; MAP1LC3A, anti-microtubule-associated protein light chain 3.

neurotransmitter-containing presynaptic vesicles and is used as a specific protein marker for the presynaptic terminal (21). Levels of synaptophysin serve as an index of synaptic number and density (22). The mean average intensity of MAP-2, GAP-43 and synaptophysin staining were significantly increased in the NSC group compared with the MCAO group (all P<0.05; Fig. 4).

Immunomodulatory properties of NSCs. The expression of IBA-1 in the microglia and GFAP in the astrocytes increase in response to a wide variety of pathological stimuli in the central nervous system (CNS). Microglia and astrocyte activation commonly occur during the early response of the CNS to a wide variety of pathological stimuli, including axotomy, trauma, inflammation and degeneration (23). There was a significant decrease in the number of IBA-1 and GFAP-positive cells in the peri-ischemic area in the NSC group compared with the MCAO group (both P<0.05; Fig. 5).

Autophagy marker levels decrease following NSC treatment. MAP1LC3 and Beclin-1 serve a pivotal role in mammalian autophagy, which is increased during periods of cell stress and extinguished during the cell cycle (24). In ischemic neurons, Beclin-1 markers were dispersed in the soma and dendrites (Fig. 6A), while MAP1LC3 was primarily located in the soma (Fig. 6B). The number of MAP1LC3-positive and Beclin-1-positive immune-reactive puncta were significantly decreased in the NSC group compared with the MCAO group (both P<0.05; Fig. 6C).

NSCs suppress ischemia-triggered inflammatory cytokines. Ischemic stroke is accompanied by increased inflammatory cytokine secretion; therefore basal cytokine secretion levels in homogenized tissue samples were measured using a protein array in which levels of different cytokines were quantified simultaneously. The secretion of pro-inflammatory cytokines, including L-selectin, leptin, MCP-1 and TNFα was increased

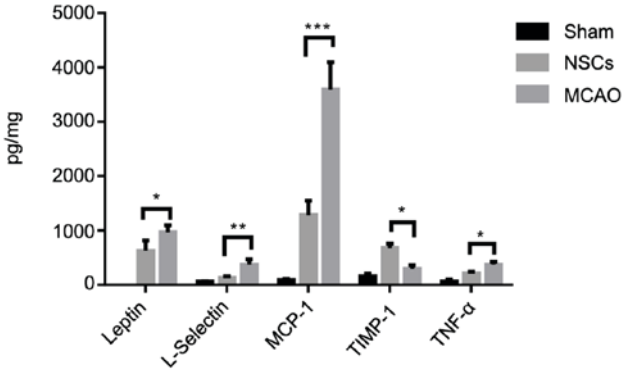

Figure 7. Cytokine analysis of brain tissues from an MCAO rat model. Among the analyzed cytokines, NSCs treatment attenuated the increase of the pro-inflammatory cytokines L-selectin, leptin, MCP-1, TNFα and further increased the release of anti-inflammatory cytokine TIMP-1. Data are presented as the mean ± standard deviation (n=5). *P<0.05, **P<0.01, ***P<0.001. MCP-1, monocyte chemotactic protein 1; TNFα, tumor necrosis factor α, TIMP-1, tissue inhibitor of metalloproteinases 1.

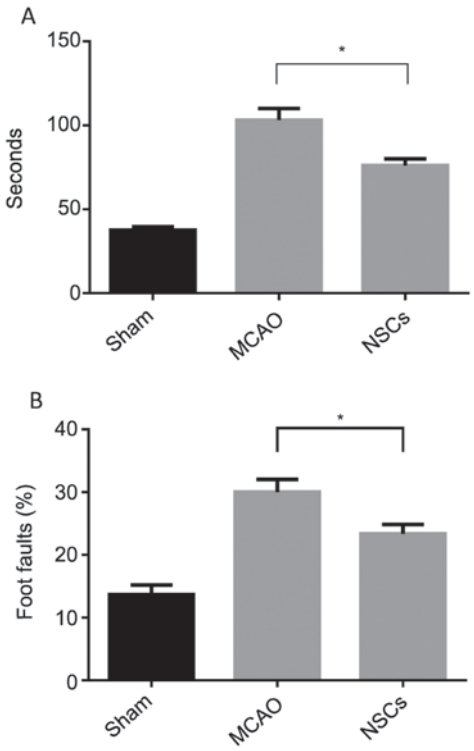

Figure 8. The results of the (A) adhesive-removal test and (B) foot-fault test 3 days following MCAO surgery. Data are presented as the mean ± standard deviation (n=7). *P<0.05. MCAO, middle cerebral artery occlusion group; NSCs, neural stem cell treatment group.

in the MCAO group compared with the sham group. NSCs further increased the release of anti-inflammatory cytokine TIMP-1 (Fig. 7). These results demonstrate that NSCs are able to shift the balance of the inflammatory response from pro-inflammatory to anti-inflammatory.

NSCs improve functional outcomes. The foot-fault and adhesive removal tests conducted 3 days following stroke onset indicated that all MCAO and MSC-treated rats exhibited severe neurological deficits. Treatment with NSCs initiated 24 h following stroke onset significantly improved performance on the adhesive removal test (P<0.05; Fig. 8A) and foot-fault test (P<0.05; Fig. 8B) compared with the MCAO group. These results indicate that NSCs may have the capacity to improve functional outcomes in mice with stroke.

Discussion

Ischemic stroke consists of a complex array of pathological processes and induces highly variable outcomes modified by many factors. The rationale for using NSCs as potential candidates in cell therapy for patients who have experienced stroke is based on a range of studies that have demonstrated or suggested the advantages conferred by NSCs following their intravenous or intracerebral administration *in vivo* through immunomodulation, signal amplification and neural repair (11,25,26). NSCs are regarded as one of the most promising stem cell candidates to be used as a therapy for many diseases where treatment is challenging (27). Patients who have experienced stroke face medical and economic burdens due to limitations in the number of available treatments (28). Stem cell based replacement therapy has therefore become attractive due to its potential to solve these problems.

In the current study, NSCs were administered to the area surrounding the lateral ventricle in the stroke-affected hemisphere. The hippocampus was identified as the ideal site for this type of intervention, as it is one of only two regions in the adult mammalian brain in which neurogenesis is ongoing (29). Furthermore, it exhibits an abundance of migration, proliferation, differentiation and integration signals (30). Thus, the hippocampus may be a potential target for treatments of neurological conditions in humans and serves as a gateway for effective clinical interventions.

Apoptosis is a specific process that leads to programmed cell death. Cytosolic cytochrome *c* release and caspase activation have been observed during ischemia-induced apoptosis (31) and NSCs are able to attenuate caspase-3 activation and impairment in OGD-treated BMECs. It has been demonstrated *in vivo* that NSCs affect the PI3K/Akt/GSK3β pathway, which regulates cell proliferation, survival and migration (14,32,33).

Ischemia increases autophagosome formation and activate autophagy. MAP1LC3 and Beclin-1 are involved in the signaling pathway that activates autophagy and the initial step of autophagosome formation (34). The *in vivo* results of the current study demonstrate that the number of MAP1LC3-positive and Beclin-1-positive immuno-reactive puncta were significantly decreased in the NSC group compared with the MCAO group. This indicates that NSCs may suppress autophagic reactions in the ischemic brain and that this role may be associated with the PI3K/Akt/GSK3β pathway, as the mechanistic target of rapamycin is downstream of this pathway and integrates signals from nutrients, energy regulators and growth factors to regulate autophagy (33).

The current study demonstrated that NSCs transplanted into the hippocampus around the ischemic boundary zone of an ischemic lesion facilitate the functional recovery from

strokes. Cell survival promoted by NSCs may contribute to this recovery. NSCs also reduce the number of GFAP and IBA1-expressing cells, which indicates that they have immunomodulatory properties. These results are consistent with those of previously published studies (9,11,26).

NSCs possess a strong anti-inflammatory capacity in a variety of disease models including Alzheimer's disease, Parkinson's disease and traumatic brain injury models (14). The current study demonstrated that NSC administration may modulate inflammation by reducing L-selectin, leptin, MCP-1 and TNFα production and increasing TIMP-1 levels.

In conclusion, the present study suggests that in addition to increasing cell survival to improve functional recovery following stroke in rats, NSCs may also activate the PI3k/Akt/GSK-3β pathway and attenuate the inflammatory process and autophagy. These effects may contribute to the underlying beneficial effects exerted by NSCs in ischemic stroke. Further investigation into the precise molecular mechanisms governing these effects may lead to the development of novel preventive and therapeutic strategies for managing ischemic injury in the future.

Acknowledgements

The authors would like to thank Shibo Wang for graphical assistance and Jiangbo Gong for proofreading.

Funding

The present study was supported by the Shanghai Pujiang Program (grant no. 18PJD058), SMMU Youth Fund (grant nos. 2017QN10, 2017QN11).

Availability of data and materials

The analyzed data sets generated during the present study are available from the corresponding author on reasonable request.

Authors' contributions

XY and XT conceived and planned the experiments, XY and XW carried out the experiments. SZ contributed to the interpretation of the results. XY took the lead in writing the manuscript. All authors provided critical feedback and helped shape the research, analysis and manuscript.

Ethics approval and consent to participate

All experimental procedures in the current study were approved by the Committee on Ethics of Biomedicine, The Second Military Medical University.

Patient consent for publication

Not applicable.

Competing interests

The authors declare that they have no competing interests.

References

1. Arsić S, Konstantinović L, Eminović F and Pavlović D: Correlation between demographic characteristics, cognitive functioning and functional independence in stroke patients. Srp Arh Celok Lek 144: 31-37, 2016.
2. Kes VB, Jurašić MJ, Zavoreo I, Lisak M, Jelec V and Matovina LZ: Age and gender differences in acute stroke hospital patients. Acta Clin Croat 55: 69-78, 2016.
3. Nentwich LM and Grimmnitz B: Neurologic emergencies in the elderly. Emerg Med Clin North Am 34: 575-599, 2016.
4. Mietto BS, Mostacada K and Martinez AM: Neurotrauma and inflammation: CNS and PNS responses. Mediators Inflamm 2015: 251204, 2015.
5. Descloux C, Ginet V, Clarke PG, Puyal J and Truttmann AC: Neuronal death after perinatal cerebral hypoxia-ischemia: Focus on autophagy-mediated cell death. Int J Dev Neurosci 45: 75-85, 2015.
6. Dugo L, Collin M and Thiemermann C: Glycogen synthase kinase 3beta as a target for the therapy of shock and inflammation. Shock 27: 113-123, 2007.
7. Yin F, Meng C, Lu R, Li L, Zhang Y, Chen H, Qin Y and Guo L: Bone marrow mesenchymal stem cells repair spinal cord ischemia/reperfusion injury by promoting axonal growth and anti-autophagy. Neural Regen Res 9: 1665-1671, 2014.
8. Zhao LR, Duan WM, Reyes M, Keene CD, Verfaillie CM and Low WC: Human bone marrow stem cells exhibit neural phenotypes and ameliorate neurological deficits after grafting into the ischemic brain of rats. Exp Neurol 174: 11-20, 2002.
9. Arien-Zakay H, Lecht S, Bercu MM, Tabakman R, Kohen R, Galski H, Nagler A and Lazarovici P: Neuroprotection by cord blood neural progenitors involves antioxidants, neurotrophic and angiogenic factors. Exp Neurol 216: 83-94, 2009.
10. Onifer SM and Low WC: Spatial memory deficit resulting from ischemia-induced damage to the hippocampus is ameliorated by intra-hippocampal transplants of fetal hippocampal neurons. Prog Brain Res 82: 359-366, 1990.
11. Roitbak T, Li L and Cunningham LA: Neural stem/progenitor cells promote endothelial cell morphogenesis and protect endothelial cells against ischemia via HIF-1alpha-regulated VEGF signaling. J Cereb Blood Flow Metab 28: 1530-1542, 2008.
12. Chou CH, Sinden JD, Couraud PO and Modo M: In vitro modeling of the neurovascular environment by coculturing adult human brain endothelial cells with human neural stem cells. PLoS One 9: e106346, 2014.
13. Committee for the Update of the Guide for the Care and Use of Laboratory Animals, Institute for Laboratory Animal Research, Division on Earth and Life Studies: Guide for the Care and Use of Laboratory Animals. 8th edition. The National Academies Press, Washington, DC, 2011.
14. Golpich M, Amini E, Hemmati F, Ibrahim NM, Rahmani B, Mohamed Z, Raymond AA, Dargahi L, Ghasemi R and Ahmadiani A: Glycogen synthase kinase-3 beta (GSK-3beta) signaling: Implications for Parkinson's disease. Pharmacol Res 97: 16-26, 2015.
15. Livak KJ and Schmittgen TD: Analysis of relative gene expression data using real-time quantitative PCR and the 2(-Delta Delta C(T)) method. Methods 25: 402-408, 2001.
16. Wang X, Yu X, Xie C, Tan Z, Tian Q, Zhu D, Liu M and Guan Y: Rescue of brain function using tunneling nanotubes between neural stem cells and brain microvascular endothelial cells. Mol Neurobiol 53: 2480-2488, 2016.
17. Schallert T, Upchurch M, Lobaugh N, Farrar SB, Spirduso WW, Gilliam P, Vaughn D and Wilcox RE: Tactile extinction: Distinguishing between sensorimotor and motor asymmetries in rats with unilateral nigrostriatal damage. Pharmacol Biochem Behav 16: 455-462, 1982.
18. Zhang R, Wang Y, Zhang L, Zhang Z, Tsang W, Lu M, Zhang L and Chopp M: Sildenafil (Viagra) induces neurogenesis and promotes functional recovery after stroke in rats. Stroke 33: 2675-2680, 2002.
19. Liu Y, Saad RS, Shen SS and Silverman JF: Diagnostic value of microtubule-associated protein-2 (MAP-2) for neuroendocrine neoplasms. Adv Anat Pathol 10: 101-106, 2003.
20. Grasselli G and Strata P: Structural plasticity of climbing fibers and the growth-associated protein GAP-43. Front Neural Circuits 7: 25, 2013.
21. Wang X, Xing A, Xu C, Cai Q, Liu H and Li L: Cerebrovascular hypoperfusion induces spatial memory impairment, synaptic changes, and amyloid-β oligomerization in rats. J Alzheimer's Dis 21: 813-822, 2010.

22. Song SH and Augustine GJ: Synapsin isoforms and synaptic vesicle trafficking. Mol Cells 38: 936-940, 2015.
23. Zhao J, Mou Y, Bernstock JD, Klimanis D, Wang S, Spatz M, Maric D, Johnson K, Klinman DM, Li X, *et al*: Synthetic oligodeoxynucleotides containing multiple telemeric TTAGGG motifs suppress inflammasome activity in macrophages subjected to oxygen and glucose deprivation and reduce ischemic brain injury in stroke-prone spontaneously hypertensive rats. PLoS One 10: e0140772, 2015.
24. Wen YD, Sheng R, Zhang LS, Han R, Zhang X, Zhang XD, Han F, Fukunaga K and Qin ZH: Neuronal injury in rat model of permanent focal cerebral ischemia is associated with activation of autophagic and lysosomal pathways. Autophagy 4: 762-769, 2014.
25. Pacey L, Stead S, Gleave J, Tomczyk K and Doering L: Neural stem cell culture: Neurosphere generation, microscopical analysis and cryopreservation. Protoc Exchange, 2006.
26. Weidenfeller C, Svendsen CN and Shusta EV: Differentiating embryonic neural progenitor cells induce blood-brain barrier properties. J Neurochem 101: 555-565, 2007.
27. Akesson E, Wolmer-Solberg N, Cederarv M, Falci S and Odeberg J: Human neural stem cells and astrocytes, but not neurons, suppress an allogeneic lymphocyte response. Stem Cell Res 2: 56-67, 2009.
28. Kankeu HT, Saksena P, Xu K and Evans DB: The financial burden from non-communicable diseases in low- and middle-income countries: A literature review. Health Res Policy Syst 11: 31, 2013.
29. Walker T, Huang J and Young K: Neural stem and progenitor cells in nervous system function and therapy. Stem Cells Int 2016: 1890568, 2016.
30. Curtis MA, Low VF and Faull RL: Neurogenesis and progenitor cells in the adult human brain: A comparison between hippocampal and subventricular progenitor proliferation. Dev Neurobiol 72: 990-1005, 2012.
31. Thiel A, Cechetto DF, Heiss WD, Hachinski V and Whitehead SN: Amyloid burden, neuroinflammation, and links to cognitive decline after ischemic stroke. Stroke 45: 2825-2829, 2014.
32. Mao Y, Ge X, Frank CL, Madison JM, Koehler AN, Doud MK, Tassa C, Berry EM, Soda T, Singh KK, *et al*: Disrupted in schizophrenia 1 regulates neuronal progenitor proliferation via modulation of GSK3beta/beta-catenin signaling. Cell 136: 1017-1031, 2009.
33. Kang EB and Cho JY: Effect of treadmill exercise on PI3K/AKT/mTOR, autophagy, and Tau hyperphosphorylation in the cerebral cortex of NSE/htau23 transgenic mice. J Exerc Nutri Biochem 19: 199-209, 2015.
34. Li H, Gao A, Feng D, Wang Y, Zhang L, Cui Y, Li B, Wang Z and Chen G: Evaluation of the protective potential of brain microvascular endothelial cell autophagy on blood-brain barrier integrity during experimental cerebral ischemia-reperfusion injury. Transl Stroke Res 5: 618-626, 2014.